

Significance of Lateral Pillar in Osteonecrosis of Femoral Head: A Finite Element Analysis

Peng-Fei Wen¹, Wan-Shou Guo^{1,2,3}, Qi-Dong Zhang², Fu-Qiang Gao², Ju-An Yue³, Zhao-Hui Liu², Li-Ming Cheng², Zi-Rong Li²

¹Department of Orthopaedic Surgery, Peking University China-Japan Friendship School of Clinical Medicine, Beijing 100029, China

²Department of Orthopaedic Surgery, Center for Osteonecrosis and Joint Preserving and Reconstruction, Beijing Key Laboratory of Arthritic and Rheumatic Diseases, China-Japan Friendship Hospital, Beijing 100029, China

³Beijing University of Chinese Medicine, Beijing 100029, China

Abstract

Background: The lateral pillar of the femoral head is an important site for disease development such as osteonecrosis of the femoral head. The femoral head consists of medial, central, and lateral pillars. This study aimed to determine the biomechanical effects of early osteonecrosis in pillars of the femoral head via a finite element (FE) analysis.

Methods: A three-dimensional FE model of the intact hip joint was constructed from the image data of a healthy control. Further, a set of six early osteonecrosis models was developed based on the three-pillar classification. The von Mises stress and surface displacements were calculated for all models.

Results: The peak values of von Mises stress in the cortical and cancellous bones of normal model were 6.41 MPa and 0.49 MPa, respectively. In models with necrotic lesions in the cortical and cancellous bones, the von Mises stress and displacement of lateral pillar showed significant variability: the stress of cortical bone decreased from 6.41 MPa to 1.51 MPa (76.0% reduction), while cancellous bone showed an increase from 0.49 MPa to 1.28 MPa (159.0% increase); surface displacements of cortical and cancellous bones increased from 52.4 μ m and 52.1 μ m to 67.9 μ m (29.5%) and 61.9 μ m (18.8%), respectively. In addition, osteonecrosis affected not only pillars but also adjacent structures in terms of the von Mises stress and surface displacement levels.

Conclusions: This study suggested that the early-stage necrosis in the femoral head could increase the risk of collapse, especially in lateral pillar. On the other hand, the cortical part of lateral pillar was found to be the main biomechanical support of femoral head.

Key words: Displacement; Finite Element Analysis; Osteonecrosis of the Femoral Head; Stress; Structure Collapse

INTRODUCTION

Osteonecrosis of the femoral head (ONFH) is highly prevalent in young adults. ONFH can result in bone collapse if not targeted with a proper and effective treatment. Such collapse can cause a requirement for hip joint replacement as seen in many Asian countries including China.^[1,2] The locale of the necrotic lesion plays an important role in the progression and treatment of ONFH.^[3] The three-pillar classification system based on the position of bone necrosis is widely accepted and used in ONFH research.^[4,5] For example, Li *et al.*^[6] reported a successful prognosis in 153 patients with nontraumatic osteonecrosis in lateral pillar of femoral head. Further, the collapse prediction rate was high in these cases. On the other hand, some studies reported a poor outcome of disease prognosis or collapse prediction rate in patients with necrotic lesions that involved the lateral pillar.^[7-9]

The collapse of femoral head has been linked to some biomechanical changes at the hip joint.^[10-12] The lateral pillar of femoral head is considered as a key factor in the prediction of collapse of ONFH, but the biomechanical studies on such matter remain limited.^[6,13] Today, there are different approaches that can correctly and effectively address clinical questions in terms of ONFH and disease

Address for correspondence: Prof. Wan-Shou Guo,

Department of Orthopaedic Surgery, Center for Osteonecrosis and Joint Preserving and Reconstruction, Beijing Key Laboratory of Arthritic and Rheumatic Diseases, China-Japan Friendship Hospital, 2 Yinghuadong Road, Chaoyang District, Beijing 100029, China
E-Mail: guowanshou@yeah.net

This is an open access article distributed under the terms of the Creative Commons Attribution-NonCommercial-ShareAlike 3.0 License, which allows others to remix, tweak, and build upon the work non-commercially, as long as the author is credited and the new creations are licensed under the identical terms.

For reprints contact: reprints@medknow.com

© 2017 Chinese Medical Journal | Produced by Wolters Kluwer - Medknow

Received: 17-07-2017 **Edited by:** Xin Chen

How to cite this article: Wen PF, Guo WS, Zhang QD, Gao FQ, Yue JA, Liu ZH, Cheng LM, Li ZR. Significance of Lateral Pillar in Osteonecrosis of Femoral Head: A Finite Element Analysis. *Chin Med J* 2017;130:2569-74.

Access this article online

Quick Response Code:



Website:
www.cmj.org

DOI:
10.4103/0366-6999.217077

progression. One important tool is finite element (FE) analysis.^[14-18] In the present study, the FE model of an intact hip joint was constructed from data extracted by images of a set of six early osteonecrosis patients and a normal control. This FE model was developed based on the three-pillar classification of ONFH. The aim of this study was to analyze the hip joint biomechanics using FE analysis when there is early osteonecrosis in different pillars of the femoral head.

METHODS

Ethical approval

The study was conducted in accordance with the *Declaration of Helsinki* and was approved by the Ethics Committee of China-Japan Friendship Hospital. Informed written consent was obtained from the participant prior to enrollment in this study.

Intact hip joint model

This study was conducted between November 2016 and June 2017 in China-Japan Friendship Hospital. An intact hip joint model was developed based on computed tomography (CT) and magnetic resonance imaging (MRI) scans of the left hip joint of a 49-year-old healthy male (170 cm, 70 kg). His bone structure was identified with CT (120 kV, 15 mA, slice thickness: 1.0 mm). Cartilage thickness (1.5 mm) was measured by MRI (echo time: 36 ms, repetition time: 1300 ms, slice thickness: 1.0 mm, and flip angle: 90°). Three-dimensional reconstruction and editing of the hip joint model were conducted in Mimics 17.0 and 3-Matic 9.0 *in silico* (Materialise Ltd., Leuven, Belgium). The data of initial graphics exchange specification exported from Mimics were processed into Rapidform XOR3 (INUS Technology, Inc., Seoul, Korea) to form solid models. These solid models were then imported into the FE analysis software Abaqus/Standard 6.14 (Dassault Systemes Simulia Corp., Providence, RI, USA) for assembling [Figure 1a]. Cartilage and cortical and cancellous bones were modeled as linear elastic isotropic materials, as previously described [Table 1].^[18,19] The cartilage-bone interface was modeled as fully bonded.

Three-dimensional models based on three-pillar classification of osteonecrosis of the femoral head

Coronal section of the femoral head was divided into three pillars by two parallel lines to femoral neck axis: lateral (30%), central (40%), and medial (30%) pillars. The pathogenesis of ONFH was identified with its location on these pillars.^[6,13] Such two-dimensional plane classification formation was followed when constructing a three-dimensional model of femoral heads with ONFH [six samples in total; Figure 1b]. Lateral, central, and medial pillars of “both” necrotic cancellous and cortical bones of femoral head were modeled as L1, C1, and M1, respectively. Lateral, central, and medial pillars of “only” necrotic cancellous bones were modeled as L2, C2, and M2, respectively. Femoral head bones with early-stage

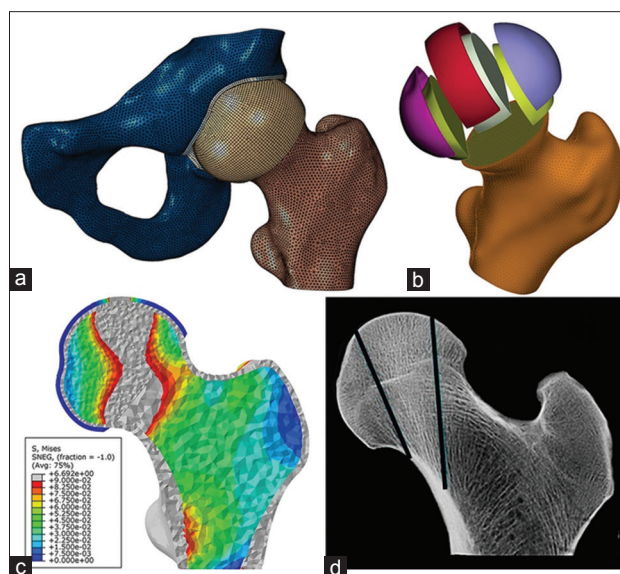


Figure 1: Numerical model of an intact hip joint (a). Regions of a three-dimensional finite element model based on three-pillar classification (b). The stress transfer path of the proximal femur (c). Radiograph of the femoral head (d).

Table 1: Material properties incorporated into the finite element models

Type of tissues	Young's modulus (MPa)	Poisson's ratio
Acetabular bone (cortical/cancellous) ^[18]	17,000.0/70.0	0.30/0.20
Femur (cortical/cancellous) ^[18]	15,100.0/445.0	0.30/0.22
Cartilage bone ^[19]	10.5	0.45
Early necrotic femur ^[18]	332.9	0.30

necrosis were modeled as linear elastic isotropic material, as previously described [Table 1].^[18,19] Interfaces between necrotic bones and cartilage or normal bones were also modeled as fully bonded.

Load and boundary conditions

As reported previously, single-limb support (mid-stance phase) of a patient was accepted as 30% of the gait cycle in this study.^[18] A compressive axis load of 570 N, which counts for 5/6 of 70 kg body weight, consistent with the load magnitude in former studies, was applied to the nodes of proximal acetabular bone.^[18,20] In addition, the muscle contractile forces around the proximal femur were not considered. For boundary conditions, constraints were applied to the X- and Y-direction displacements of the nodes on the symphysis pubis.^[19] Nodes on distal end of the femur were completely fixed to prevent any translation and rotation. The contact surface between acetabular and femoral head cartilages was defined with a friction coefficient of 0.01.^[20]

Finite element analysis

For each model, FE analysis was performed using the Abaqus/Standard 6.14 software. Cancellous and cortical bones were meshed by 10-node tetrahedral elements in each

model, and cartilages were meshed by hexahedral elements with an approximate element size of 1–2 mm [Figure 1a]. Fine FE meshes of 541,783 elements and 227,583 nodes were used in the FE modeling. In necrotic lesions, relatively dense meshes were used. Sensitivity analyses showed that increasing element density failed to impact the prediction accuracy of the model, but did increase the computational load by the nature of the explicit FE method. A convergence test was conducted to verify the selected element size mesh quality; accordingly, the analysis was performed on the element size of the femur to ensure that peak von Mises stress does not change over 5%. The von Mises stress and surface displacement in the cancellous and cortical bones were calculated and analyzed in each of the FE models.

Validation of intact hip joint model

FE analyses were evaluated by the comparison of obtained principal stress transfer paths and the contact pressure distributions of the present study to relevant previous reports with *in vitro* experimentation. In the present analysis, the concentrated pressure region was accepted in the anterolateral part of the femoral head, and the maximum contact pressure value (2.65 MPa) was similar to Bae's report (2.45 MPa).^[18] Characteristics of the principal stress transfer are important for the biomechanical index. In Figure 1c, the principal stress distribution from the top of the femoral head to calcar was illustrated in healthy hip joint model; such simulation results were found consistent with the results of previous studies.^[19,21] In addition, the shape and location of the biomechanical transfer path were consistent with the distribution of bone density [Figure 1d]. Thus, we hypothesized that the FE results could reflect the physical status of the hip and could be used to analyze the effects of the early osteonecrosis that occur in different pillars of the femoral head.

RESULTS

Displacement and equivalent stress (the von Mises stress)

Figure 2 shows the von Mises stress distributions of cortical and cancellous bones as well as displacement cloud map in all models. The maximum stress of 0.50 MPa (cortical bone) and 0.06 MPa (cancellous bone) was set uniformly in the von Mises stress distributions to achieve a relevant distribution that can be compared within each other. In Figure 2a and 2b, panels exhibited the concentrated pressure regions that were located in the anterolateral part of the femoral head in all the six three-dimensional geometric models of ONFH. Moreover, stress distributions showed a remarkable change in L1 and C1 models. The peak stress in the cortical and cancellous bones decreased markedly as shown in L1 models [Figure 2a], whereas cancellous bone alone showed an increase in L2 and C2 models [Figure 2b]. Surface displacements were substantially altered in the weightbearing area of models L1, C1, and M1 [Figure 2c].

Change variable values of displacement

Change values of peak displacement of the lateral pillars and necrotic lesions, stress indices, and peak stresses of necrotic lesions for all models are listed in Table 2. Accordingly, change values of peak displacement of the lateral pillars for L1, C1, and M1 models were higher than L2, C2, and M2 counterparts. Necrotic lesions of different pillars also showed higher change values of peak displacement in cortical bone models. On the other hand, the stress index of necrotic lesion in L1 model (0.275) was higher than 0.100. Likewise, the peak stress of necrotic lesion in L1 model (1.51 MPa) was higher than the critical stress (0.51 MPa).

Changes in the peak von Mises stress and displacement

The peak values of von Mises stress of cortical and cancellous bones were 6.41 MPa and 0.49 MPa, respectively [Figure 3a].

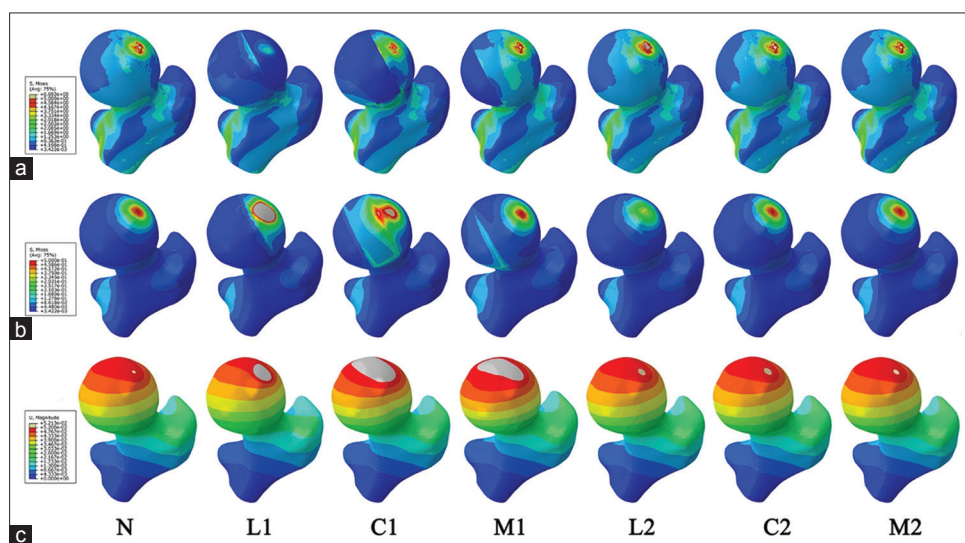


Figure 2: The von Mises stress distribution of the models on the surface of femoral cortical (a) and cancellous (b) bones. (c) Displacement cloud map in femoral head of the models. Models were represented as follows: L1 (lateral), C1 (central), and M1 (medial) pillars of necrotic cortical and cancellous bones of femoral head. L2, C2, and M2 represent same pillars for only necrotic cancellous bone of femoral head.

In the lateral pillar of L1 model, the peak von Mises stress of necrotic cortical bone decreased from 6.41 MPa to 1.51 MPa (76.0% reduction), whereas the same value for cancellous bone increased from 0.49 MPa to 1.28 MPa (159.0% increase). Both regions strikingly exceeded the critical stress level (0.55 MPa). The peak von Mises stresses of cortical and cancellous bones of central pillars were 0.45 MPa and 0.51 MPa in C1 models, respectively [Figure 3a]. Such values in necrotic cortical bone decreased by 89.0%, whereas increased by 108.0% compared to control values, and both results were close to those of critical stress [Figure 3a]. In other three-dimensional ONFH models, the von Mises stress of necrotic lesions showed smaller values than the critical stress.

In the intact hip joint model (normal control), peak values of displacement were 52.4 μm of L1, 51.1 μm of C1, 48.0 μm of M1, 52.1 μm of L2, 50.4 μm of C2, and 46.8 μm of M2 [Figure 3b]. In the lateral pillar of L1 model, the peak displacement of necrotic cortical and cancellous bones showed an increase from 52.4 μm and 52.1 μm to 67.9 μm (29.5%) and 61.9 μm (18.8%), respectively. In L2 model, the peak displacement of necrotic cortical and cancellous bones of central pillar increased from 51.1 μm and 50.4 μm to

56.5 μm (10.6%) and 56.4 μm (11.9%), respectively. Finally, there was a decreased trend of displacement changes from L1 to M1 models, but the displacement changes were small among L2, C2, and M2 models [Figure 3b].

DISCUSSION

Osteonecrosis in femoral head results in bone degeneration and hip joint dysfunction in most individuals; surgery becomes inevitable in a majority of these cases.^[9] Till now, there is no standard treatment for patients with early-stage ONFH. The treatment strategy depends on a number of factors such as the necrosis classification and volume.^[6,9] Gao *et al.*^[9] reported that the extracorporeal shock wave therapy generated poor outcomes in most patients with osteonecrosis involving the lateral pillar (335 patients, 528 hips). Ma *et al.*^[8] showed that porous tantalum implant surgery combined with bone grafting is not an adequate option for ONFH treatment, especially in patients involving the lateral pillar. Zuo *et al.*^[7] analyzed clinical factors that related to the failure of bone grafting through a window at the femoral head-neck junction and found that patients with necrotic lesions involving the lateral pillar showed high surgical failure rates. Such studies proved that the collapse of the early-stage ONFH was mainly due to biomechanical instability caused by the microfracture of the trabecular bone in the necrotic region. Today, a large body of FE studies focused on the impact of necrosis volume on the collapse progression, but studies considering the three-pillar classification are rare.

In this study, femoral cortical bone conferred a vital role for load bearing in all FE models, and such finding was consistent with the results reported by Brown *et al.*^[22] The peak value of von Mises stress in the femoral cortical bone (6.41 MPa) was strikingly higher than that in the cancellous counterpart (0.49 MPa). In Brown's study, the stress transfer of the ONFH through an FE method showed that the stress of the center of necrosis region decreased markedly. In turn, the necrosis lesion on a subchondral bone facilitated the collapse of the femoral head.^[22] This phenomenon might be caused by the decreased yield strength of necrotic bone, and femoral head lacked a

Table 2: Change variable values of peak displacement, stress indices, and peak von Mises stress

Models	Change value of peak displacement (μm)		Stress index of necrotic lesion*	Peak stress of necrotic lesion (MPa)
	Lateral pillar	Necrotic lesion		
L1	15.51	15.51	0.275	1.51
C1	4.83	5.40	0.093	0.51
M1	2.25	3.75	0.039	0.22
L2	0.42	0.42	0.065	0.36
C2	0.40	0.29	0.037	0.21
M2	0.16	0.22	0.023	0.13

*Stress index = effective stress/yield strength. Microfractures form in necrotic lesions when the stress index is >0.1 and the peak stress is higher than the critical stress (0.55 MPa). Models were represented as follows: L1 (lateral), C1 (central), and M1 (medial) pillars of necrotic cortical and cancellous bones of femoral head. L2, C2, and M2 represent same pillars for only necrotic cancellous bone of femoral head.

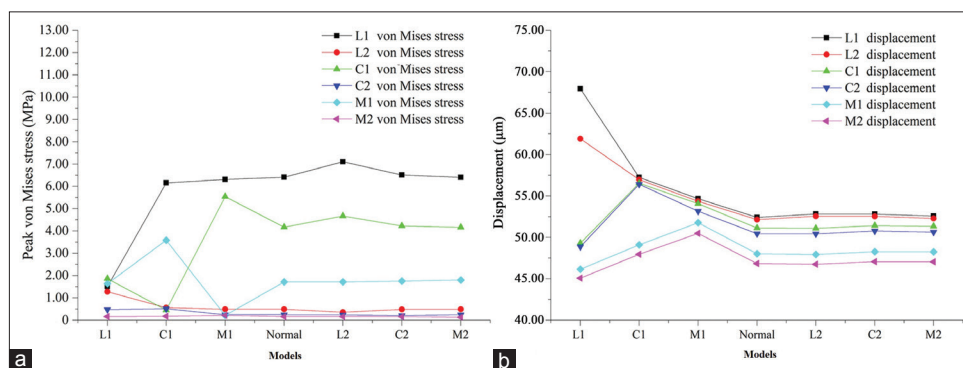


Figure 3: The peak von Mises stress (a) and displacement (b) of necrotic lesions in three pillars of femoral head in the models. Models were represented as follows: L1 (lateral), C1 (central), and M1 (medial) pillars of necrotic cortical and cancellous bones of femoral head. L2, C2, and M2 represent same pillars for only necrotic cancellous bone of femoral head.

normal mechanical support due to decreased elastic modulus.^[23]

The early-stage necrosis in femoral head can result in bone collapse, probably because of microfractures in the necrotic lesion. Local microfractures occur in bone tissue when the peak von Mises stress exceeds the yield strength. Stress is an important determinant in the bone modeling/remodeling process. A weaker yield strength of necrotic bone can expand microfractures until bone collapse. Yang *et al.*^[23] reported that the yield strength of necrotic tissue was 5.5 MPa, which was defined by the ratio of effective stress and yield strength, called the stress index. In theory, yield or fracture occurs when the stress index is >0.100 ; hence, the critical stress should be 0.55 MPa.^[24] A region where $>50\%$ of it shows an effective stress level higher than the critical stress is likely to collapse. In contrast, if this area is $<50\%$ of the total lesion, only decompensated microfractures will occur and fail to collapse the bone.

Another important finding of the present study was that the early osteonecrosis in lateral pillar of femoral head exhibited the highest risk of collapsing; this was probably due to the concentrated stress located at the top of the stress transfer path in the lateral pillar.^[14,18,25] In L1 model, the peak von Mises stress of lateral pillar of cortical and cancellous bones was 1.51 MPa and 1.28 MPa, respectively. The stress index of necrotic lesion (0.275) was markedly higher than 0.100. As a consequent, the lateral pillar of femoral head could easily collapse under such stress condition. In addition, the peak displacement was increased with the change value of 15.51 μm [Table 2]. In C1 model, the peak von Mises stress and stress index of cortical and cancellous bones showed similar levels to those of the critical stress and stress index. Thus, the central pillar had a low risk of collapse under the load condition of a normal weight; nevertheless, the risk level for collapsing would increase under loading levels of routine activity such as walking downstairs or accidental stumbling. Differences were small in other three-dimensional ONFH models, and the stress index and peak stress were smaller than the yield criteria. Accordingly, the risk of collapse was expected to be low in M1, L2, C2, and M2 models.

The present results indicated that the peak von Mises stress and displacement in adjacent structures of necrotic pillar were affected in all models. The adjacent normal bone tissue might bear the burden caused by the necrotic area; for example, results of central and medial pillars were similar in the L1 model, but lateral and medial pillar results were altered in C1 model. As shown in Table 2, the change value of the peak displacement in lateral pillar was 4.83 μm in C1 model. Such influences did not reach significance in other three-dimensional ONFH models. In L1 and C1 models, the noticeable internal interaction was possibly because the necrotic lesions involved the subchondral bone.

One of the limitations of the present study was that the structure of the FE models was specific to the volunteer's

formation as constructed from the data of CT and MRI images. The structure of normal control hip joint was simplified for FE analysis, and ligaments, capsules, and musculatures of hip joint were not taken into consideration. In addition, the material property of the bone structure was considered as linear elastic and homogeneous for simplification, which might have caused some alteration in the natural behavior of bone. Till now, it is well known that the cortical and cancellous bones contain spatial inhomogeneity in their properties. Another limitation was that the ideal three-dimensional ONFH models would hardly reflect the complicated necrotic tissue structure of patients in clinical perspective. To obtain a more precise biomechanical analysis, other ONFH models should be tested as a future direction. The condition of static loading was built on only one loading state of normal walking (30% of the gait cycle) in the present study. For more accurate evaluation, FE analysis should be conducted using the loading states of walking downstairs and accidental stumbling.

In conclusion, six osteonecrosis of femoral head geometrical FE models were constructed in this study. Such modeling has demonstrated that the femoral head showed the highest collapse risk in L1 model (lateral pillar of cortical and cancellous bones), because of the increase in the peak von Mises stress and displacement. Another important finding was that the lateral pillar of the cortical bone was the main biomechanical support of femoral head. As a result, the lateral pillar of cortical bone also played an important role in the disease progression. This study introduced a theoretical biomechanical basis for the hip preservation treatment in early osteonecrosis of femoral head.

Financial support and sponsorship

This study was supported by grants from the National Natural Science Foundation of China (No. 81673776), and the Capital Health Research and Development of Special (No. 2016-2-4062).

Conflicts of interest

There are no conflicts of interest.

REFERENCES

1. Zhao DW, Yu M, Hu K, Wang W, Yang L, Wang BJ, *et al.* Prevalence of nontraumatic osteonecrosis of the femoral head and its associated risk factors in the Chinese population: Results from a nationally representative survey. *Chin Med J* 2015;128:2843-50. doi: 10.4103/0366-6999.168017.
2. Ma JH, Guo WS, Li ZR, Wang BL. Local administration of bisphosphonate-soaked hydroxyapatite for the treatment of osteonecrosis of the femoral head in rabbit. *Chin Med J* 2016;129:2559-66. doi: 10.4103/0366-6999.192768.
3. Kang JS, Moon KH, Kwon DG, Shin BK, Woo MS. The natural history of asymptomatic osteonecrosis of the femoral head. *Int Orthop* 2013;37:379-84. doi: 10.1007/s00264-013-1775-y.
4. Herring JA, Neustadt JB, Williams JJ, Early JS, Browne RH. The lateral pillar classification of Legg-Calvé-Perthes disease. *J Pediatr Orthop* 1992;12:143-50. doi: 10.1097/01241398-199203000-00001.
5. Rajan R, Chandrasenan J, Price K, Konstantoulakis C, Metcalfe J, Jones S, *et al.* Legg-Calvé-Perthes: Interobserver and intraobserver reliability of the modified herring lateral pillar classification. *J Pediatr Orthop* 2013;33:120-3. doi: 10.1097/BPO.0b013e318277d047.

6. Li Z, Liu Z, Sun W, Shi Z, Wang B, Zhao F, *et al.* The classification of osteonecrosis of the femoral head based on the three pillars structure: China-Japan Friendship Hospital (CJFH) classification. *Chin J Orthop* 2012;32:515-20. doi: 10.3760/cma.j.issn.0253-2352.2012.06.001.
7. Zuo W, Sun W, Zhao D, Gao F, Su Y, Li Z, *et al.* Investigating clinical failure of bone grafting through a window at the femoral head neck junction surgery for the treatment of osteonecrosis of the femoral head. *PLoS One* 2016;11:e0156903. doi: 10.1371/journal.pone.0156903.
8. Ma J, Sun W, Gao F, Guo W, Wang Y, Li Z. Porous tantalum implant in treating osteonecrosis of the femoral head: Still a viable option? *Sci Rep* 2016;6:28227. doi: 10.1038/srep28227.
9. Gao F, Sun W, Li Z, Guo W, Wang W, Cheng L, *et al.* High-energy extracorporeal shock wave for early stage osteonecrosis of the femoral head: A Single-center case series. *Evid Based Complement Alternat Med* 2015;2015:468090. doi: 10.1155/2015/468090.
10. Hong G, Han X, Fang B, Zhou G, He W, Chen L. Finite element analysis applied to the diagnosis and treatment of osteonecrosis of femoral head: Latest progress (in Chinese). *Chin J Tissue Eng Res* 2017;21:450-5. doi: 10.3969/j.issn.2095-4344.2017.03.023.
11. Yu T, Xie L, Chu F. A sclerotic rim provides mechanical support for the femoral head in osteonecrosis. *Orthopedics* 2015;38:e374-9. doi: 10.3928/01477447-20150504-53.
12. Tran TN, Warwas S, Haversath M, Classen T, Hohn HP, Jäger M, *et al.* Experimental and computational studies on the femoral fracture risk for advanced core decompression. *Clin Biomech (Bristol, Avon)* 2014;29:412-7. doi: 10.1016/j.clinbiomech.2014.02.001.
13. Herring JA, Kim HT, Browne R. Legg-Calve-Perthes disease. Part I: Classification of radiographs with use of the modified lateral pillar and Stulberg classifications. *J Bone Joint Surg Am* 2004;86-A:2103-20. doi: 10.2106/00004623-200410000-00001.
14. Liu WG, Wang SJ, Yin QF, Liu SH, Guan YJ. Biomechanical supporting effect of tantalum rods for the femoral head with various sized lesions: A finite-element analysis. *Chin Med J* 2012;125:4061-5. doi: 10.3760/cma.j.isn.0366-6999.2012.22.027.
15. Floerkemeier T, Lutz A, Nackenhorst U, Thorey F, Waizy H, Windhagen H, *et al.* Core decompression and osteonecrosis intervention rod in osteonecrosis of the femoral head: Clinical outcome and finite element analysis. *Int Orthop* 2011;35:1461-6. doi: 10.1007/s00264-010-1138-x.
16. Shi J, Chen J, Wu J, Chen F, Huang G, Wang Z, *et al.* Evaluation of the 3D finite element method using a tantalum rod for osteonecrosis of the femoral head. *Med Sci Monit* 2014;20:2556-64. doi: 10.12659/MSM.890920.
17. Alonso-Rasgado T, Jimenez-Cruz D, Bailey CG, Mandal P, Board T. Changes in the stress in the femoral head neck junction after osteochondroplasty for hip impingement: A finite element study. *J Orthop Res* 2012;30:1999-2006. doi: 10.1002/jor.22164.
18. Bae JY, Kwak DS, Park KS, Jeon I. Finite element analysis of the multiple drilling technique for early osteonecrosis of the femoral head. *Ann Biomed Eng* 2013;41:2528-37. doi: 10.1007/s10439-013-0851-1.
19. Zhou G, Zhang Y, Zeng L, He W, Pang Z, Chen X, *et al.* Should thorough debridement be used in fibular allograft with impaction bone grafting to treat femoral head necrosis: A biomechanical evaluation. *BMC Musculoskelet Disord* 2015;16:140. doi: 10.1186/s12891-015-0593-3.
20. Yang B, Liu Y, Liu S. Necrosis of the femoral head treated by tantalum rod implant: Three-dimension finite element analysis (in Chinese). *Chin J Tissue Eng Res* 2016;20:1295-301. doi: 10.3969/j.issn.2095-4344.2016.09.012.
21. Xiao D, Ye M, Li X, Yang L. Development of femoral head interior supporting device and 3D finite element analysis of its application in the treatment of femoral head avascular necrosis. *Med Sci Monit* 2015;21:1520-6. doi: 10.12659/msm.893354.
22. Brown TD, Mutschler TA, Ferguson AB Jr. A non-linear finite element analysis of some early collapse processes in femoral head osteonecrosis. *J Biomech* 1982;15:705-15. doi: 10.1016/0021-9290(82)90024-0.
23. Yang JW, Koo KH, Lee MC, Yang P, Noh MD, Kim SY, *et al.* Mechanics of femoral head osteonecrosis using three-dimensional finite element method. *Arch Orthop Trauma Surg* 2002;122:88-92. doi: 10.1007/s004020100324.
24. Fang B, He W, Zhan L, Zhang Q, Wei Q, Chen Z, *et al.* Finite element analysis of stress distribution over femoral head necrosis zones in different necrosis areas. *J Tradit Chin Orthop Traumatol* 2012;24:10-5. doi: 10.3969/j.issn.1001-6015.2012.10.003.
25. Zhao D, Qiu X, Wang B, Wang Z, Wang W, Ouyang J, *et al.* Epiphyseal arterial network and inferior retinacular artery seem critical to femoral head perfusion in adults with femoral neck fractures. *Clin Orthop Relat Res* 2017;475:2011-23. doi: 10.1007/s11999-017-5318-5.